J. Gubicza[a,b], I. C. Dragomir[b], G. Ribárik[b], S. C. Baik[c], Y. T. Zhu[d], R. Z. Valiev[e], T. Ungár[b]

[a] Department of Solid State Physics, Eötvös University, Budapest, Hungary
[b] Department of General Physics, Eötvös University, Budapest, Hungary
[c] Institute for Materials Engineering and Technology, University of Technology, Clausthal, Germany
[d] Materials Science and Technology Division, Los Alamos National Laboratory, Los Alamos, NM, USA
[e] Institute of Physics of Advanced Materials, Ufa State Aviation Technical University, Ufa, Russia

Dislocation structure and crystallite size distribution in plastically deformed Ti determined by X-ray peak profile analysis

Ultrafine-grained titanium produced by equal channel angular pressing and subsequent cold rolling is studied by X-ray diffraction. It is found that a texture exists in which the hexagonal basal planes are parallel to the longitudinal axis of the billet. The crystallite size distribution and the dislocation structure are determined by X-ray diffraction peak profile analysis. The median and the variance of the crystallite size distribution are obtained as $m = 39$ nm and $\sigma = 0.14$, respectively. The dislocation model of anisotropic broadening of peak profiles enables to determine the active slip systems. It was found that all three possible hexagonal Burgers vectors of dislocations exist, with the composition of 66 % <*a*> type, 33 % <*c*> type and 1 % <*c* + *a*> type.

Keywords: Crystallite size distribution; Dislocation structure; Ti; Severe plastic deformation; X-ray peak profile analysis

1. Introduction

Severe plastic deformation (SPD) techniques, e. g. equal channel angular pressing (ECAP) and high-pressure torsion (HPT), are effective for producing fully dense, bulk ultrafine-grained (submicron-grain-sized or nanostructured) materials [1]. The nanomaterials produced by SPD techniques have an attractive combination of high strength and good ductility due to their 100 % density, low contamination and unique nanostructures [2–4]. A two-step SPD process, ECAP followed by cold rolling, has recently been developed to obtain high strength in nanostructured, commercially pure Ti [5]. The ECAP was conducted at 400–450 °C since Ti lacks sufficient ductility at lower temperatures. The warm ECAP processing increased the yield strength of commercially pure Ti by 68 % [2] to 640 MPa, and the cold rolling at room temperature further increased the yield strength to over 900 MPa [4, 5] while maintaining a strain to failure of 9.2 % under tensile load. One of the most significant features of the stress–strain curves of nanostructured Ti is the lack of strain hardening.

The first step to understand the mechanical behavior of nanostructured Ti produced by ECAP is to characterize its microstructure. This can be done locally by transmission electron microscopy (TEM) or in large volume of the material by X-ray diffraction peak profile analysis. X-ray diffraction peak profiles are broadened due to small crystallite sizes and/or lattice distortions. The two effects can be separated on the basis of the different diffraction order dependence of peak broadening. The standard methods of peak profile analysis based on the full widths at half maximum (FWHM), the integral breadths and the Fourier coefficients of the profiles provide the apparent crystallite size and the mean square strain [6–8]. The evaluation of the broadened peak profiles is complicated by strain anisotropy. This means that neither the FWHM nor the integral breadth nor the Fourier coefficients of the profiles are monotonous functions of the diffraction vector [9, 10]. It has been shown that strain anisotropy can be well accounted for by the dislocation model of the mean square strain by introducing the contrast factors of dislocations [11–15]. Since the values of the dislocation contrast factors depend on the dislocation slip systems present in the crystal, the evaluation of X-ray profiles for the contrast factors enables the determination of the dislocation structure. In the last few years, fast development in the computer technique makes it possible to work out procedures that can determine the parameters of the microstructure by fitting the whole diffraction profiles [16–20]. In the recently elaborated multiple whole profile (MWP) fitting method, the Fourier coefficients of the measured physical profiles are fitted by the Fourier coefficients of the theoretical functions of size and strain peak profiles [19, 20]. This procedure enables the determination of crystallite size distribution and the dislocation structure in nanostructured materials.

In this paper, the microstructure, i. e. the texture, crystallite size, size distribution and dislocation structure, evolved during the SPD processing (ECAP + cold rolling) of Ti sample was studied by X-ray diffraction peak profile analysis.

2. Experimental details

An ultrafine-grained titanium specimen was produced by a two-step SPD procedure. In the first step, a Ti billet with an average grain size of 10 μm was deformed by warm ECAP using a 90° die following route B_C for 8 passes

[1,5]. The dimensions of the billet were 25 mm in diameter and 100 mm long. The specimen contained the following impurities (in wt.%): 0.12 O, 0.01 H, 0.04 N, 0.07 C and 0.18 Fe. The temperature of warm ECAP was 450 °C at the first pass, but droped to 400 °C after 8 passes. Molybdenum disulphide was used as lubricant. In the second step, the specimen processed by ECAP was further deformed by cold rolling at room temperature to further improve the strength. During cold rolling, the initial Ti billet had a circular cross-section with a diameter 16 mm and was deformed into square cross-section with edges of approximately 11 mm. The reduction in cross-section area of the billet was 73 %. The detailed description of the four-step cold-rolling procedure is given in Ref. [5].

A longitudinal section and a cross-section were prepared for X-ray diffraction. In order to avoid machining effects, an approximately 100 μm surface layer was removed from the specimen surface by chemical etching before the X-ray experiments. The diffractograms for the two sections were measured by a Philips X'pert diffractometer using a Cu anode and a pyrolitic graphite secondary monochromator. The X-ray diffraction peak profile analysis was carried out on the following eight peaks: 00.2, 01.1, 10.3, 00.4 reflections from the longitudinal-section and 01.0, 11.0, 20.0, 02.1 reflections from the cross-section. These profiles were also measured by a high-resolution double-crystal diffractometer (Nonius, FR 591) using Cu Ka_1 radiation. The instrumental broadening of the double-crystal diffractometer ($\Delta(2\Theta)_{instr} = 0.012^0$) is negligible, compared to the physical peak broadening for the ultrafine-grained titanium ($\Delta(2\Theta)_{phys} = 0.4-0.6^0$). Therefore, no instrumental corrections were applied. The peak profiles were evaluated by the MWP fitting procedure described in details in Refs. [19, 20]. In this method, the Fourier transform of the experimental profiles are fitted by the product of the theoretical Fourier transforms of size and strain peak profiles [19, 20].

The theoretical functions used in the fitting are calculated on the basis of a microstructural model. In this model, the crystallites have a spherical shape and a log-normal size distribution, and the lattice strains are assumed to be caused by dislocations. The analysis involves the following steps: (i) the Fourier coefficients of the experimental profiles were calculated by a non-equidistant sampling Fourier transformation; (ii) The theoretical Fourier coefficients of the size and strain profiles were calculated for a set of microstructural parameters; (iii) The experimental and the calculated Fourier coefficients were compared by the least-squares method. The procedure has six fitting parameters for hexagonal crystals: (i) the median and the variance, m and σ, of the log-normal size distribution function, (ii) the density and the arrangement parameter of dislocations, ρ and M, and (iii) the q_1 and q_2 parameters in the contrast factors of dislocations. The value of M gives the strength of the dipole character of dislocations: the higher M value corresponds to weaker dipole character and weaker screening of the displacement fields of dislocations. From the values of q_1 and q_2 the relative fractions of the $<a>$, $<c>$ and $<c + a>$-type Burgers vectors in the dislocation population are determined by a procedure described in Ref. [21]. The arithmetic, the area- and the volume-weighted mean crystallite sizes are obtained from σ and m using formulas given in Ref. [22]. The texture was examined by pole figures measured by X-ray diffraction on the longitudinal section of the sample.

3. Results and discussion

The X-ray diffractograms obtained from the longitudinal section and cross-section are shown in Figs. 1a and b, respectively. The difference between the relative intensities of the diffraction peaks in the two diffractograms reveals strong texture in the sample. The 00.l diffraction peaks are missing in the diffractogram obtained from the cross-section. This means that all the hexagonal basal planes are parallel to billet longitudinal axis. This texture can be also seen in the pole figures of the 10.0 and 00.2 reflections shown in Figs. 2a and b, respectively. The texture developed in the two-step SPD procedure is similar to the *t*-type texture often appeared in cold rolled hexagonal materials [23]. In this type of texture the (00.1) poles are tilted from the normal direction (ND) of the rolled surface towards the transverse direction (TD) and the (10.0) poles are parallel to the rolling direction (RD). The formation of similar texture in the ECAP processed Ti billets has been also observed by other authors [2]. The cold rolling in the two-step SPD procedure could further enhance this texture.

The 01.0, 01.1 and 11.0 reflections, which have high intensities in both powder diffractograms in Fig. 1, were used to investigate crystallite shape anisotropy. The normalized intensities of these peaks are compared in Figs. 3a–c. The good agreement between the profiles obtained from the two different sections indicates that there is no crystallite shape anisotropy with respect to the billet axis. This obser-

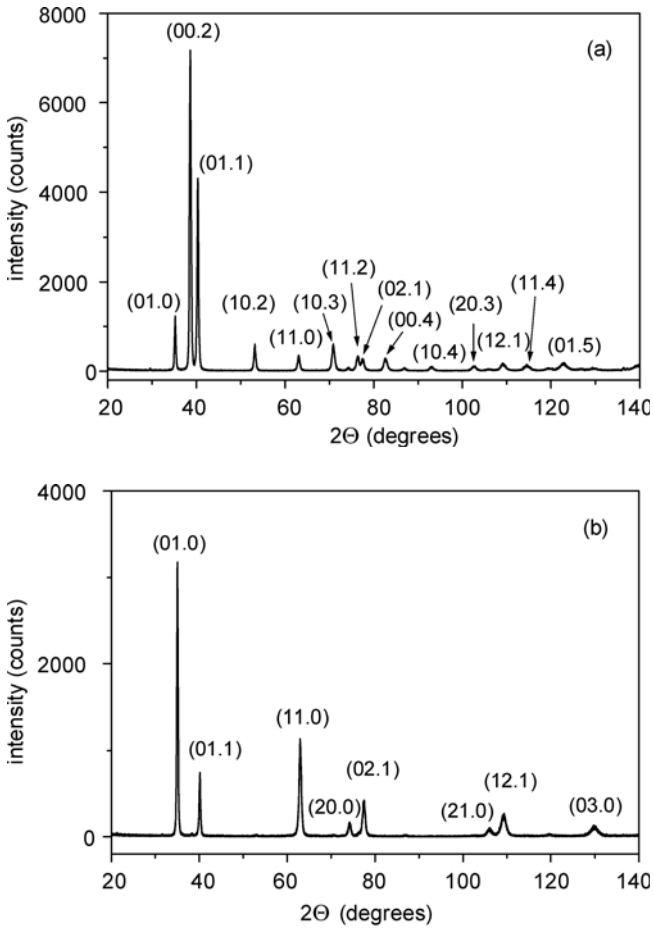

Fig. 1. X-ray diffractograms obtained from (a) the longitudinal section and (b) the cross-section.

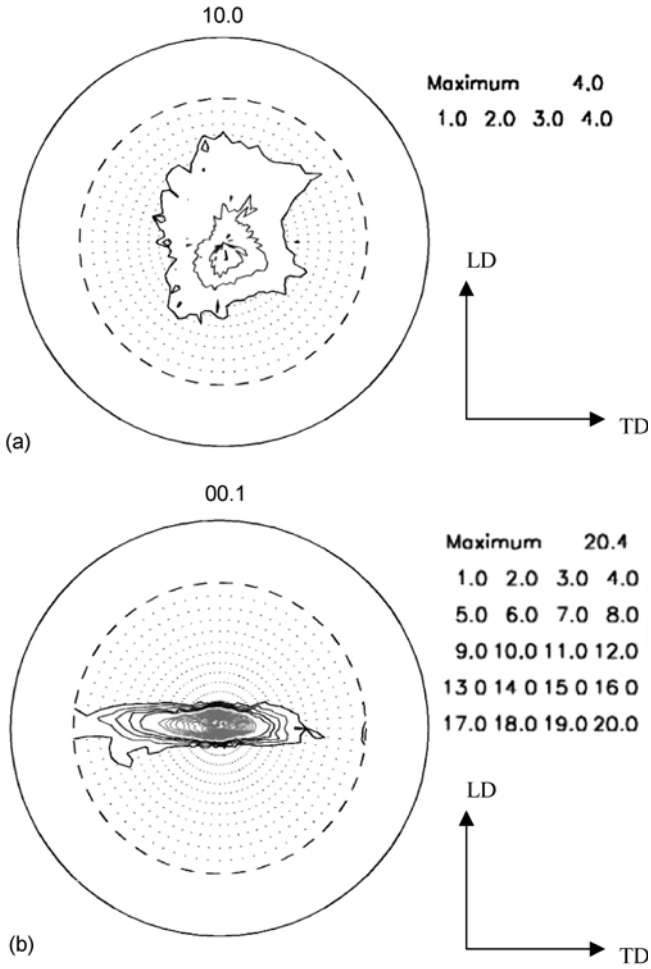

Fig. 2. The pole figures for the 10.0 (a) and the 00.1 (b) reflections. LD – longitudinal direction, TD – transverse direction.

vation is also supported by previous TEM investigations on another warm ECAP processed commercially pure Ti specimen [2].

The X-ray diffraction profiles obtained by high-resolution measurements were evaluated by the MWP method described in Section 2. The measured and the fitted Fourier coefficients are shown in Fig. 4. The difference between the measured and the fitted values are also shown in the figure. The weighted least-squares error (R_{wp}) is 4 % where the weights are the reciprocal of the observed Fourier transforms. The microstructural parameters obtained from the fitting are: $m = 39 \pm 4$ nm, $\sigma = 0.14 \pm 0.03$, $\rho = 3 \pm 0.6 \cdot 10^{15}$ m^{-2}, $M = 3.1 \pm 0.4$, $q_1 = -1.16 \pm 0.09$ and $q_2 = -0.60 \pm 0.08$. The arithmetic, the area- and the volume-weighted mean crystallite sizes calculated from the values of m and σ are 39 ± 6, 41 ± 6 and 42 ± 6 nm, respectively.

The crystallite size distribution according to the m and σ values obtained from X-ray diffraction is plotted in Fig. 5. The area-weighted mean size is also marked in the figure. It can be established that the severe plastic deformation of Ti resulted in nanocrystalline structure. The microstructure of the Ti specimen processed by warm ECAP and cold rolling was also investigated by TEM [24]. A good correlation is found between the area-weighted mean crystallite size determined from X-ray diffraction (41 nm) and the mean

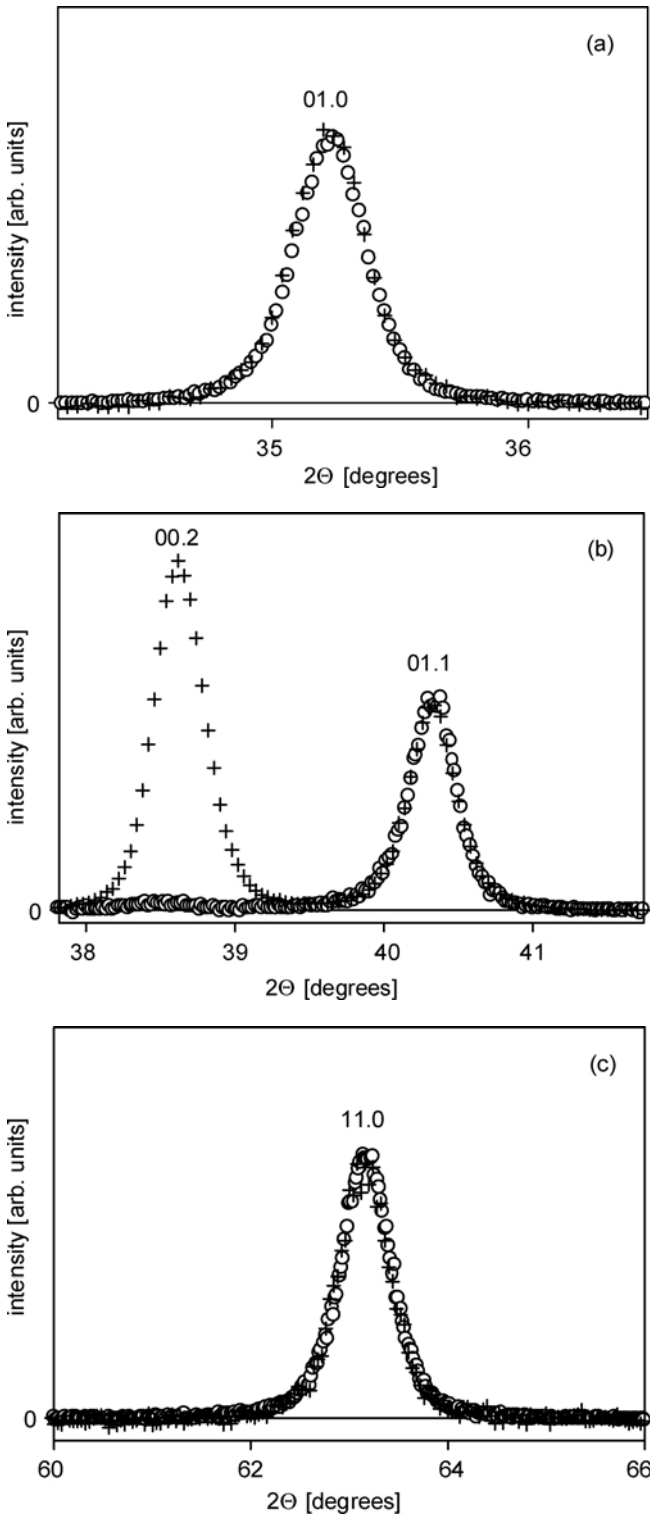

Fig. 3. Comparison of the diffraction profiles obtained from the longitudinal section (denoted by crosses) and the cross-section (denoted by open circles) for the reflections 01.0 (a), 01.1 (b) and 11.0 (c).

size of the dislocation cells (45 nm) obtained from TEM micrographs [24]. It should be noted however, that the grain size is much higher, 265 nm, according to the averaging over 150 grains in the TEM micrographs [24]. This is consistent with previous observations for SPD processed materials [19], since the coherently scattering domains measured by X-rays is the smallest one in the size-hierarchy of the objects (dislocation cell, subgrain, grain) in deformed metals.

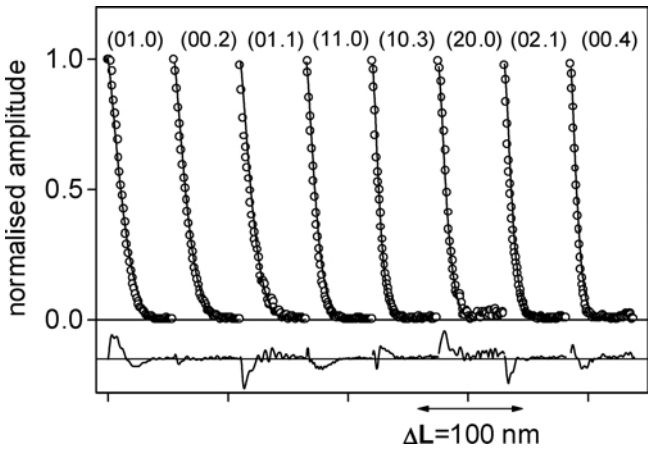

Fig. 4. The measured and fitted Fourier coefficients normalized to unity. The differences between the measured and fitted values are also shown in the lower part of the figure. The scaling of the differences is the same as in the main part of the figure. The indices of the reflections are also indicated.

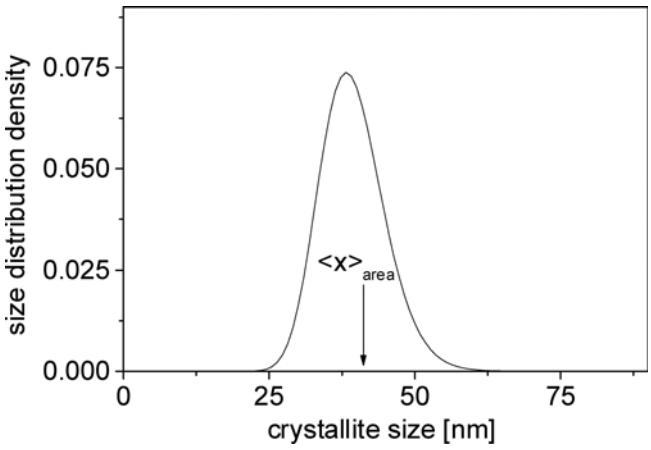

Fig. 5. The crystallite size distribution density function and the area-weighted mean size determined from X-ray peak profile analysis.

The q_1 and q_2 parameters of the contrast factors depend on the character of dislocations, and therefore enable the determination of the prevailing dislocation slip systems in the sample. The q_1 and q_2 values for the eleven possible slip systems in Ti according to Kuzel and Klimanek [14] have been calculated and listed in Table 2 in Ref. [21]. The experimental q_1 and q_2 values for Ti do not match any single pair of the q_1 and q_2 parameters calculated theoretically. This indicates that more than one dislocation slip systems have been activated during deformation. A recently elaborated numerical procedure [21] was applied to determine the Burgers vector population in the ECA pressed + cold-rolled Ti. In a hexagonal crystal, three Burgers vector types exist: $b_1 = 1/3\langle 11\bar{2}0\rangle$ (<*a*> type), $b_2 = \langle 0001\rangle$ (<*c*> type) and $b_3 = 1/3\langle 11\bar{2}3\rangle$ (<*c* + *a*> type). The eleven dislocation slip systems can be classified into three groups based on their Burgers vectors: <*a*> type: BE, BS, PrE, PyE; <*c*> type: Pr2E, PrS; <*c* + *a*> type: Pr3E, Py2E, Py3E, Py4E, Py2S where B, Pr, Py, E and S denote the basal, the prismatic, the pyramidal slip systems, the edge and the screw dislocations, respectively. The detailed list of the dislocation slip systems in Ti is presented in Ref. [21]. The relative fraction of each type of dislocations can be calculated by making the measured and the weighted averaged theoretical values of q_1 and q_2 equal [21]. According to this calculation the Burgers vector population is obtained as:

<*a*>-type dislocations: 66 (8) %,

<*c*>-type dislocations: 33 (5) %,

<*c*+*a*>-type dislocations: 1 (1) %.

The dislocation structure in plastically deformed titanium has been extensively studied by TEM [25–30]. These works reported the abundance of <*a*>-type dislocations besides the <*c*>- and <*c*+*a*>-type dislocations, which agrees very well with our X-ray results.

4. Conclusions

The microstructure of ultrafine-grained titanium produced by SPD (warm ECAP + cold rolling) has been studied by X-ray peak profile analysis. It is established that a texture exists in which hexagonal basal planes are parallel to billet longitudinal axis. It is found that SPD produces mean crystallite size of several tens of nanometers (well below 100 nm). The crystallite size value determined by X-rays is in good agreement with the dislocation cell size obtained by TEM. The dominant Burgers vector of dislocations observed in titanium is <*a*> type which correlates well with previous TEM observations.

Thanks are due to Dr R. J. Hellmig for his kind assistance in performing the texture measurements. This work was supported by the Hungarian Scientific Research Fund, OTKA, Grant Nos. T031786, T034666 and T029701 as well as the NIS-IPP program in the US Department of Energy. J.G. is grateful for the financial support of Magyary Zoltán Postdoctoral Programme of Foundation for Hungarian Higher Education and Research (AMFK). Y.T.Z. and R.Z.V. acknowledge the support of US DOE IPP program.

References

[1] R.Z. Valiev, R.K. Ishlamgaliev, I.V. Alexandrov: Progr. Mater. Sci. 45 (2000) 103.
[2] V.V. Stolyarov, Y.T. Zhu, I.V. Alexandrov, T.C. Lowe, R.Z. Valiev: Mater. Sci. Eng. A 299 (2001) 59.
[3] V.V. Stolyarov, Y.T. Zhu, I.V. Alexandrov, T.C. Lowe, R.Z. Valiev: Mater. Sci. Eng. A 303 (2001) 82.
[4] D. Jia, Y.M. Wang, K.T. Ramesh, E. Ma, Y.T. Zhu, R.Z. Valiev: Appl. Phys. Lett. 79 (2001) 611.
[5] V.V. Stolyarov, Y.T. Zhu, I.V. Alexandrov, T.C. Lowe, R.Z. Valiev: Mater. Sci. Eng. A 343 (2003) 43.
[6] G.K. Williamson, W.H. Hall: Acta Metall. 1 (1953) 22.
[7] B.E. Warren, B.L. Averbach: J. Appl. Phys. 21 (1950) 595.
[8] B.E. Warren: Progr. Metal Phys. 8 (1959) 147.
[9] G. Caglioti, A. Paoletti, F.P. Ricci: Nucl. Instrum. 3 (1958) 223.
[10] A. Le Bail: in E. Prince, J.K. Stalick (Eds.), Accuracy in Powder Diffraction II, NIST Special Publication, Washington DC, No. 846 (1992) 142.
[11] M.A. Krivoglaz: Theory of X-ray and Thermal Neutron Scattering by Real Crystals, Plenum Press, New York (1996).
[12] M. Wilkens: Phys. Stat. Sol. (a) 2 (1970) 359.
[13] M. Wilkens, in: J.A. Simmons, R. de Wit, R. Bullough (Eds.), Fundamental Aspects of Dislocation Theory, Vol. II, Nat. Bur. Stand. (US) Spec. Publ. No. 317, Washington, DC (1970) 1195.
[14] R. Kuzel jr., P. Klimanek: J. Appl. Cryst. 22 (1989) 299.
[15] T. Ungár, A. Borbély: Appl. Phys. Lett. 69 (1996) 3173.
[16] D. Balzar: J. Res. Nat. Inst. Stand. Technol. 98 (1993) 321.
[17] J.I. Langford, D. Louër, P. Scardi: J. Appl. Cryst. 33 (2000) 964.
[18] P. Scardi, M. Leoni: Acta Cryst. A 58 (2002) 190.
[19] T. Ungár, J. Gubicza, G. Ribárik, A. Borbély: J. Appl. Cryst. 34 (2001) 298.
[20] G. Ribárik, T. Ungár, J. Gubicza: J. Appl. Cryst. 34 (2001) 669.
[21] I.C. Dragomir, T. Ungár: J. Appl. Cryst. 35 (2002) 556.

[22] W.C. Hinds: Aerosol Technology: Properties, Behavior and Measurement of Airbone Particles, Wiley, New York (1982).
[23] S. Zaefferer: Mater. Sci. Eng. A 344 (2003) 20.
[24] Y.T. Zhu, J.Y. Huang, J. Gubicza, T. Ungár, Y.M. Wang, E. Ma, R.Z. Valiev: J. Mater. Res., to be submitted.
[25] I.P. Jones, W. B. Hutchinson: Acta Metall. 29 (1981) 951.
[26] S. Naka, A. Lasalmonie, P. Costa, L.P. Kubin: Phil. Mag. A 57 (1988) 717.
[27] S. Farenc, D. Caillard, A. Couret: Acta Metall. Mater. 41 (1993) 2701.
[28] A.R. Smirnov, V.A. Moskalenko: Mater. Sci. Eng. A 327 (2002) 138.
[29] D.R. Chichili, R.K.T. Ramesh, K.J. Hemker: Acta Mater. 46 (1998) 1025.
[30] A. Girschick, D.G. Pettifor, V. Vitek: Phil. Mag. A 77 (1998) 999.

(Received March 03, 2003)

Correspondence address

Prof. Tamas Ungar
Department of General Physics
Eotvos University
Budapest, P. O. Box 32, H-1518, Hungary
Tel.: +36 1 372 2801
Fax: +36 1 372 2811
E-mail: ungar@ludens.elte.hu